Tellus (1983), *35A*, 256–268

An investigation of summer sea surface temperature anomalies in the eastern North Pacific Ocean

By JOHN R. LANZANTE and ROBERT P. HARNACK, *Department of Meteorology and Physical Oceanography, Cook College, New Jersey Agricultural Experimental Station, Rutgers, The State University of New Jersey, New Brunswick, N.J. 08903, U.S.A.*

(Manuscript received April 5; in final form November 22, 1982)

ABSTRACT

A study of summer sea surface temperature anomalies in the eastern North Pacific Ocean was undertaken to examine some of the processes that could affect their evolution and which may be important for their prediction. An empirical approach was utilized. The factors considered include sea surface temperature (SST) persistence (due to the relatively large heat capacity of the water), oceanic thermal advection, and wind mixing (which presumably acts through changes in the mixed layer depth of the ocean). The primary variable studied was the summer SST anomaly for each of 25, 5° latitude by 10° longitude boxes in the region 140° W–170° E, 30–55° N. Thirty years of data were used (1947–76).

Diagnostic analyses using data from four Ocean Weather Stations (C, D, P and V) were performed prior to the analyses described above in order to examine wind mixing more closely. Only at the OWS's are high frequency (3 hour), measured wind speeds available at the same location as SST observtions for a long period of time. These analyses indicated a statistically significant lag relationship between average April and May monthly wind speed and subsequent summer SST at Station P.

The monthly mean SLP gradient was used as an estimate of average monthly wind speed over the 25 box domain where measured winds are not routinely available. In addition, winds derived from daily sea level pressure (SLP) analyses were averaged to form monthly means. At most boxes, no significant lag relationship between summer SST anomalies and spring (April and May) winds was found using either wind data set.

The box-averaged data were employed to specify the summer SST from the components of the total horizontal thermal advection (based on the mean and anomalous components of the surface current and SST fields). The anomalous summer surface current advecting the mean summer SST field was found to be the dominant horizontal advective term affecting the local time rate of change of SST, particularly for 40–50° N. Substitution of derived May anomalous currents for those of summer greatly diminished the strength of the relationship.

In the predictive portion of the study, skill relative to persistence was marginal based upon dependent sample testing. Thus, in the *predictive mode* neither wind mixing (as parameterized here) nor oceanic thermal advection added very much information not contained in the initial SST anomaly field. However, persistence alone exhibited considerable skill, particularly in the northeastern portion of the domain.

1. Introduction

The quest for a more complete understanding of ocean–atmosphere interactions has accelerated in recent years. Much effort has been devoted to relating midlatitude oceanic thermal patterns with prior, concurrent, and subsequent atmospheric fields. Namias (1959, 1965, 1972, 1976) has been the chief proponent of the theory that anomalies of vertical fluxes of latent and sensible heat, which arise due to an abnormal sea surface temperature (SST) distribution, result in anomalies of the atmospheric circulation. Davis (1978) found evidence of a significant statistical lag relationship (during summer and autumn) in which the ocean leads the atmosphere. Furthermore, local changes in the atmosphere may induce remote changes (i.e., atmospheric teleconnections).

A study by Namias (1976), in which the summer SST pattern in the eastern North Pacific was related to the Aleutian low in autumn, has been examined here with particular interest. Namias' study suggests that the successful prediction of summer SST could lead to skillful predictions of the intensity of the Aleutian low during autumn. The spatial domain used in this study (170° E–140° W, 30–55° N) has been chosen with these ideas in mind.

The objectives of this study are both diagnostic and predictive. First, the relative importance and spatial variability of various predictors of summer SST were examined individually. Next, an attempt was made to skillfully predict area-averaged summer SST anomalies from spring oceanic and atmospheric parameters. Because of the intimate relationship between ocean and atmosphere, both media must be considered in the prediction of either. Regression analysis with prior SST, oceanic thermal advection, and wind parameters as predictors was utilized.

The first step in this study was to examine the lag effect of upper oceanic wind mixing during spring on the subsequent summer SST anomaly, proposed here to act in part through changes in the mixed layer depth. This proposal is supported by the work of Camp and Elsberry (1978), Elsberry and Raney (1978), and Elsberry and Camp (1978) who examined the relationship between the cube of the friction velocity and SST changes. These studies indicate that the greater the wind mixing, the deeper the mixed layer and the lower the SST. The analysis, reported in Section 3.1, was carried out using data reported at very short time intervals ($\sim$ hours) for a long time span, ($\sim 10^1$ years) which are only available at the Ocean Weather Stations (OWS's). Next, the magnitude of the monthly SLP gradient vector was used as an estimate of the average monthly wind speed and was computed over the entire domain. This procedure was necessary since regularly *measured* wind speed values are available only at the OWS's. Estimated winds from daily sea level pressure analyses, which became available later, were also used.

In a further diagnostic analysis (Section 3.2), the effect of oceanic thermal advection on the summer SST anomaly field was investigated. In the past, numerous investigators have incorporated some form of oceanic thermal advection to either predict or specify SST anomalies. Early diagnostic studies such as those by Namias (1959), Eber (1961) and Namias (1965) established the importance of advection (of the long-term mean component of the SST field by the anomalous Ekman drift) in determining the evolution of SST anomaly fields on the time scale of a month to a season. Modifictions and the addition of more physical processes were made in follow-up studies by Arthur (1966), Jacob (1967) and Clark (1972). In recent years, more complex thermodynamic numerical models have been utilized (Adem, 1970a, b; Haney et al., 1978; Haney, 1980). However, these investigations have generally been performed on a case study basis.

It was the intent here to examine oceanic thermal advection using a relatively large sample (30 cases). The relative importance of the various components of advection was also examined. In addition, comparisons between advection calculations for specification and prediction were made. The analyses of Section 3 were done for the purpose of diagnostic examination of each of the predictors separately before formulating the final predictive models. Finally, in Section 4, regression models were formed and were evaluated in terms of hindcast skill and significance.

2. Data employed

Some of the parameters used in this study were basic (such as mean ocean currents, measured wind speed, SLP, and SST) while others were derived from the basic data sets. The latter include the magnitude of the SLP gradient vector (used as a measure of average monthly wind speed) and the anomalous wind-induced surface currents, derived from the SLP field.

The data used include monthly SST (1947–76), on a 5° latitude by 5° longitude grid, provided by the Scripps Institution of Oceanography, and monthly SLP (1947–76) on a 10° latitude by 10° longitude grid, from the National Center for Atmospheric Research (NCAR). Both are on magnetic tape. Mean summer ocean currents were estimated using a set of atlases (Department of the Navy Oceanographic Office, 1977), which are summaries of all available surface current observations (from the 1850s to the mid-1970s). The observtions were summarized by 1° × 1° squares and by months in four atlases that cover the study area. Observations from June, July, and August were used to compute a long-term summer mean for each of 25, 5° × 10° boxes in the domain (140° W–170° E, 30–55° N).

A magnetic tape of wind speed and direction for April and May was provided by the Fleet Numerical Oceanographic Central (FNOC). The wind vectors on this tape were derived (by FNOC) from six hourly analyses of northern hemisphere SLP. Six hourly wind speeds were extracted covering the domain of this study.

In the single station analyses, data from four magnetic tapes of atmospheric and oceanic parameters, measured every three hours at four ocean weather stations (OWS's), were used. These tapes were acquired from the National Climatic Center (NCC) in Asheville, NC. The stations used are: "C" (1945–73; 53° N, 35° W), "D" (1950–72; 44° N, 41° W), "P" (1944–78; 50° N, 145° W) and "V" (1953–71; 33° N, 160° E). In the subsequent analyses, all available OWS data were utilized in order to make the sample size as large as possible.

3. Diagnostic studies of predictors of summer SST

3.1. *The effect of upper oceanic wind mixing*

The surface mixed layer, which lies between the ocean surface and the thermocline, is the primary participant in air–sea interactions. Because of its strong static stability, the thermocline effectively separates the layer below it from surface effects on a short time scale (~days). In midlatitude regions, seasonal variations in the vertical structure of the upper ocean can be explained largely by seasonal variations of convective mixing (caused by surface cooling), and wind mixing (due to storms), which follow the annual heating cycle. The usual result is a much deeper mixed layer in the cold season than in the warm season.

Elsberry and Garwood (1978) established the importance of wind mixing on the mixed layer depth and SST during the warm season by investigating the spring transition from a deep to a shallow mixed layer. If this transition occurs earlier than normal, net radiative gains will be confined to a shallow layer for a longer than normal period of time, resulting in a positive SST anomaly. Conversely, a later than normal transition leads to a negative SST anomaly. In further studies, Elsberry and Camp (1978), Camp and Elsberry (1978), and Elsberry and Raney (1978) examined the relationship between U_*^3 (where U_* is the friction velocity, the cube of which is an indicator of the mechanical generation of turbulent kinetic energy) and changes in SST at OWS's P, N and V. It was found that a disproportionately small number of "wind events" (occurring ~5% of the time) accounted for the major part (~50%) of the accumulated monthly totals of U_*^3; in addition, "wind events" occurring 15–19% of the time accounted for one third of the net change in SST during the same month. Elsberry and Raney concluded that during the heating season (March–August), SST increases occur during periods of light winds rather than during periods of above normal insolation.

In the light of these findings, it seems natural to include a measure of the character of the mixed layer in a model used to predict warm season, mid-latitude SST. It is proposed here that wind data during April and May will render some information concerning the spring transition date from a deep to a shallow mixed layer. The transition date cannot be routinely determined except at a limited number of locations (primarily OWS's) where bathythermograph observations are taken regularly. The transition, which has a mean date of occurrence of April 27 at OWS P (and a range of 70 days) is highly correlated with SST averaged over the period March through December (Elsberry and Garwood, 1978). Thus, the relationship between April and May wind speeds and summer SST is sought.

Given that the mean transition date at OWS P is in late April and roughly a month sooner at OWS V, the relationship sought here may not be due entirely to the mechanism in which prior wind mixing determines the date of transition. It may be that for some time after the initial transition, the shallow mixed layer is readily subjected to temporary deepening, as determined by the degree of wind mixing. However, as the warm season progresses, climatological influences (acting through increased solar radiation which enhances static stability) make disruption of the mixed layer increasingly difficult. It should be kept in mind that although subsequent to the spring transition, mixed layer depth increases are less likely, and shorter lived than before, they still may occur. Thus, a significant relationship between a *wind parameter* and *summer SST* may be due to (1) the dependence of the "transition date" on *prior* wind mixing as well as (2) the vertical redistribution of thermal energy *subsequent* to the spring transition.

Before proceeding to the predictive state of this study, the association between April and May winds and summer SST was examined more closely. Since both measured SST and wind speed data are desired at very short sampling intervals, for a long time span, virtually all sources except the OWS's were eliminated. Based on the length of their data bases, four OWS's were chosen; there are two each in the Atlantic (C and D) and Pacific (P and V). Although OWS's C and D are outside the primary area of interest of this study, they were selected for use in diagnostic analysis because of their relatively long data bases.

The summer SST was computed by averaging all June, July, and August observations. The raw observations of wind speed (available every three hours) were transformed into daily averages for each day of April and May. The daily values were used to compute monthly wind speed parameters of the form:

$$(1/n) \sum_{i=1}^{n} W_i^p \qquad (1)$$

where p varies from 1 to 4, W_i is the daily wind speed for day i of either April or May and n is the number of days in the month. As p increases, high speed events, which account for most of the monthly change in SST (Elsberry and Camp, 1978; Elsberry and Raney, 1978), are weighted more. Allowing p to vary from 1 to 4 was primarily an empirical choice designed to facilitate a comparison between a parameter which is more greatly influenced by high wind speed events ($p = 4$) with one that weights all wind events equally ($p = 1$). Table 1 shows the correlation coefficient of summer SST with both May SST and the wind speed parameters (for April and May) at each of the OWS's used.

The expected sign of the correlation is positive for SST (highly persistent) and negative for the wind parameters (mixed layer deepening effect). Negative correlations between summer SST and the spring wind parameters are found at all OWS's during May and at P and V during April, indicating that greater than normal wind speeds are followed by higher than normal summer SST. Except for OWS V in May, as the power (p) decreases the correlation generally becomes more negative. The opposite was expected since higher p values weight strong wind mixing events proportionately more. It appears that the monthly mean wind speed relates better to summer SST than do the other wind parameter types. Although significance was found primarily at one OWS (P), this should not discourage one from trying to use the wind parameters for prediction in the eastern North Pacific since "P" is the only OWS located there. One would not expect the wind mixing process to be as important at the Atlantic OWS's (C and D) because of the relatively greater surface heat fluxes there than at OWS P as shown by estimates made

Table 1. *Correlations of summer SST at ocean weather stations (C, D, P and V) with monthly (April and May) SST and wind parameters. Sample size (n) and 5% significance level are also given. Underlined values are significant at the 5% level*

	April				May			
	C	D	P	V	C	D	P	V
SST	−.020	.355	<u>.427</u>	<u>.491</u>	.354	.427	<u>.737</u>	<u>.600</u>
$\sum w/n$	.119	.048	−<u>.504</u>	−.453	−.336	−.308	−<u>.698</u>	−.257
$\sum w^2/n$	.136	.026	−<u>.489</u>	−.434	−.298	−.275	−<u>.644</u>	−.320
$\sum w^3/n$	.142	−.004	−<u>.449</u>	−.392	−.267	−.233	−<u>.599</u>	−.361
$\sum w^4/n$	.143	−.038	−<u>.389</u>	−.343	−.244	−.182	−<u>.511</u>	−.380
n	29	23	32	19	29	23	32	19
5% level	.377	.428	.358	.475	.377	.428	.358	.475

by Barnett (1978), using the work of Budyko (1955).

At this point, it might be argued that while wind mixing does influence SST (at least at OWS P), the effect is evidenced entirely in the SST of the same month and that no *lag* effect is present. For an example of a lag effect, consider the case of an early transition. Normal climatological solar heating leads to a greater than *normal* increase of SST with time. This increase in SST would not be evidenced right at the time of transition. Alternatively, spring winds may influence *only* spring SST (with no *lag* effect acting through anomalies in the mixed layer depth); the relationsip then would be due to persistence of spring SST into summer.

In order to eliminate the influence of persistence of SST from April or May to summer, the partial correlation (Brooks and Carruthers, 1978) between spring wind parameters and summer SST, holding the SST of the same month (as the wind parameters) constant, has been computed (Table 2). The partial correlation (which is based upon the simple correlations between the variables involved) is a statistic which measures the correlation between two variables, eliminating the effect(s) of any other variable(s). While the partial correlation coefficients tend to be smaller in magnitude than the simple ones, the overall conclusions remain the same. A significent statistical relationship between both April and May mean wind speeds and summer SST exists at OWS P. Thus, there is reason to believe that April and/or May monthly mean wind speeds may be a useful predictor of eastern North Pacific summer SST. Only at OWS V, with $p = 1$, is the correlation more negative during April than May. Perhaps this is due to a transition date about a month earlier than at P, as suggested by maps of long-term average monthly mixed layer depth for the Pacific Ocean, prepared by Bathen (1972).

The use of daily (or more frequent) *measured* wind speed values in oceanic regions in a predictive scheme is not practical since such observations can only be found at the OWS's, which are few in number. As a matter of practicality, the magnitude of the monthly mean SLP gradient vector, normalized by latitude (to account for variations in the coriolis parameter) was used as a measure of the monthly mean wind speed. While some information may have been lost in this substitution, it is a great simplification. It was encouraging that the correlation between the magnitude of the May SLP gradient (at 40–50° N, 140–150° W) and summer SST at OWS P (−0.656) is nearly as great as that between the measured wind speed (at OWS P) and summer SST there (−0.698).

Next, the relationship between the SLP gradient parameter and summer SST was examined over the entire region of interest. The monthly anomalous SLP gradients for April and May (SLPA and SLPM, respectively) were correlated with the change in SST anomaly from May (SSTM) to summer (SSTS). The SLP gradient and SST anomalies were computed as the average over each of 25 boxes (5° latitude by 10° longitude) as shown in Fig. 1. The correlations, which are shown in Table 3 are small, although they generally have the expected sign (negative). However, only one of the negative correlations is significant at the 5% level.

Because of the poor results shown in Table 3, a wind data set (on a 63 × 63 grid covering the entire northern hemisphere) was obtained in order to replace the monthly SLP gradient anomaly (on a 10° × 10° grid) as a measure of oceanic wind mixing. A magnetic tape of *estimated* April and

Table 2. *Partial correlation between summer SST and April and May wind parameters holding SST of the same month constant. Correlations significant at the 5% level are also given (underlined)*

	April				May			
	C	D	P	V	C	D	P	V
$\sum w/n$	.117	.096	−.<u>394</u>	−.460	−.316	−.286	−.<u>476</u>	−.394
$\sum w^2/n$	.135	.078	−.<u>381</u>	−.439	−.288	−.247	−.<u>362</u>	−.427
$\sum w^3/n$	.141	.049	−.356	−.393	−.264	−.203	−.288	−.440
$\sum w^4/n$	.143	.015	−.320	−.339	−.243	−.153	−.161	−.436
5% level	.377	.428	.358	.475	.377	.428	.358	.475

May wind vectors, derived from hemispheric SLP analyses available every six hours from 1947–76, was obtained from the Fleet Numerical Oceanographic Central. This data set was not utilized initially because of the much greater cost of processing 6 hourly as opposed to monthly data. Box-averaged wind speeds, as well as wind frequencies, were computed every six hours utilizing all data within each box.

As was the case when OWS data were used, the correlation between the wind parameters (of the form $(1/n) \sum_{i=1}^{n} W_i^p$) and the May to summer SST anomaly change was better (i.e., more negative) when $p = 1$ than when $p = 2$ or $p = 3$. The correlations (not shown) using the best of a variety of wind frequency parameters are only slightly better than when the magnitude of the anomalous SLP gradient was used (Table 3). However, in both cases a significant relationship is not evident overall.

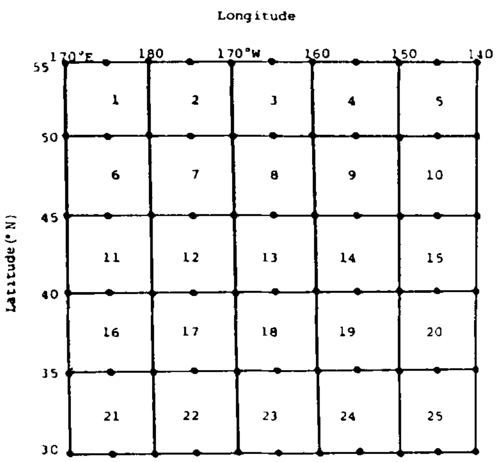

Fig. 1. Diagram of the 25 boxes used in the prediction of summer SST. Dots indicate SST data gridpoints. Six gridpoint values of SST comprise each box average.

3.2. *The effect of oceanic thermal advection*

Another physical process that was considered in this study (in addition to wind mixing and SST persistence) is near surface oceanic thermal advection. In the past, a number of investigators have used some form of oceanic thermal advection to either predict or specify SST anomalies. In a diagnostic study, Namias (1959) used anomalous Ekman transport (derived from the anomalous SLP field) to advect the long-term mean SST distribution. He found that computed magnitudes of SST anomalies were much too large, and that there was also some discrepancy between actual and computed patterns. Follow-up studies by Eber (1961) and Namias (1965) in which actual (rather than normal) SST was advected gave better results. However, these studies involved a limited number of cases.

Arthur (1966) suggested a further modification of Namias' scheme using a perturbation analysis,

Table 3. *Correlations between anomalous April (top) and May (bottom) SLP gradient (SLPA and SLPM, respectively) and summer minus May SST anomaly change. All quantities are box averaged. Correlations larger in magnitude than 0.355 (underlined) are significant at the 5% level*

Latitude	170° E–180	180–170° W	170° W–160	160–150	150–140
55–50	.041	−.196	−.042	−.127	−.036
	−.160	−.307	−.079	−.039	−.411
50–45	−.042	.179	.038	.053	−.109
	.034	−.025	−.223	−.224	−.228
45–40	.079	.052	.011	−.042	−.096
	−.014	.061	−.082	−.183	−.140
40–35	−.142	−.202	−.317	.122	.469
	−.081	−.062	.131	.339	.172
35–30	−.138	−.206	−.200	.171	.356
	−.185	−.263	−.073	−.112	−.028

the results of which are reported by Jacob (1967). This analysis is one in which the advective term $\mathbb{W}\cdot\nabla T$ (where $\mathbb{W}$ = actual ocean surface current and T = actual SST) is decomposed into its mean and fluctuating components. Thus:

$$\mathbb{W} = \bar{\mathbb{W}} + \mathbb{W}' \tag{2}$$

$$T = \bar{T} + T' \tag{3}$$

where the bar denotes a long-term mean (monthly or seasonal) and the prime denotes a deviation from the mean (i.e., monthly or seasonal anomaly). Substituting and expanding the advective term yields:

$$\mathbb{W}\cdot\nabla T = \bar{\mathbb{W}}\cdot\nabla T' + \mathbb{W}'\cdot\nabla\bar{T} + \mathbb{W}'\cdot\nabla T' + \bar{\mathbb{W}}\cdot\nabla\bar{T} \tag{4}$$

The four terms (from left to right) represent advection of the anomalous SST by the normal current, advection of the normal SST by the anomalous component of the surface current, advection of the anomalous SST by the anomalous component of the surface current, and advection of the normal SST by the normal surface currents. The last term is a constant and does not enter into a study of interannual variability. Hereafter, the first three terms on the right-hand side will be referred to as advection types 1, 2 and 3 (ADV1, ADV2 and ADV3), respectively. It will be convenient to treat these three terms separately in the predictive models because of the different ways in which the currents and SST's are computed or estimated for each.

The initial state for advection types 1 ($\bar{\mathbb{W}}\cdot\nabla T'$) and 3 ($\mathbb{W}'\cdot\nabla T'$) is the anomalous May SST field. The mean summer ocean currents which were used to compute $\bar{\mathbb{W}}\cdot\nabla T'$ are long-term mean values (Department of the Navy Oceanographic Office, 1977). The anomalous component of the surface current used to compute $\mathbb{W}'\cdot\nabla T'$ and $\mathbb{W}'\cdot\nabla\bar{T}$ was derived from the anomalous *May* SLP field using geostrophic and Ekman theory as was done by Namias (1959 and 1965), Eber (1961), Jacob (1967), and Adem (1970a, b).

The correlations between advection types 1–3 and May to summer SST anomaly change (SSTS minus SSTM), for the 25 boxes (shown in Fig. 1), based on 30 years (1947–76) are shown in Table 4. The correlations are marginal at best, with highest values between 40–50° N for type 1, 45–55° N for type 2 and 40–55° N for type 3.

In order to gain further insight into the advective process, advection types 2 and 3 were computed in the *specification* sense by using the *summer* SLP

Table 4. *Correlations between May to summer SST anomaly change (SSTS–SSTM) and (top to bottom within each box)* $\bar{\mathbb{W}}\cdot\nabla T'$, $\mathbb{W}'\cdot\nabla\bar{T}$, *and* $\mathbb{W}'\cdot\nabla T'$ *using box-averaged quantities. Values significant at the 5% lever are underlined*

Lat.	170° E – 180	180 – 170° W	170° W – 160	160 – 150	150 – 140
55–50	.156	.092	$-\underline{.500}$	.087	.289
	.115	−.211	.145	$\underline{.473}$	$\underline{.639}$
	.206	.090	−.030	$\underline{.384}$	.142
50–45	.286	$\underline{.443}$	−.022	$\underline{.493}$	.331
	−.054	.075	.341	.228	.190
	.298	$\underline{.363}$	.255	−.040	$\underline{.422}$
45–40	.306	−.004	.141	$\underline{.510}$	.228
	−.101	−.022	.187	−.029	−.043
	.235	$\underline{.357}$	.333	−.035	.209
40–35	.247	−.024	−.039	.222	−.003
	−.081	−.017	.124	−.181	−.157
	.125	.307	−.014	−.106	−.144
35–30	.132	.156	.152	.287	.301
	.145	.177	.135	.089	.044
	.234	.322	.170	−.019	.056

distribution to derive the anomalous surface currents. In actual *prediction*, the *May* SLP distribution must be used assuming some degree of persistence from May to summer. Correlations (not shown) similar to those presented in Table 4 indicate that even in specification, type 3 advection is not important. However, the correlations involving type 2 advection are much better, particularly between 40–50° N, where all the correlations are significant at the 5% level. The latitudinal dependence of the correlation coefficients is quite distinct for type 2 advection.

Fig. 2 compares the zonally-averaged correlation coefficient between type 2 advection ($W' \cdot \nabla\bar{T}$) and May to summer SST anomaly change for specification (solid) with that of prediction (dashed). The curve for specification indicates quite clearly the importance of type 2 advection, particularly between 40–50° N, in the evolution of the summer SST anomaly field. This, along with the

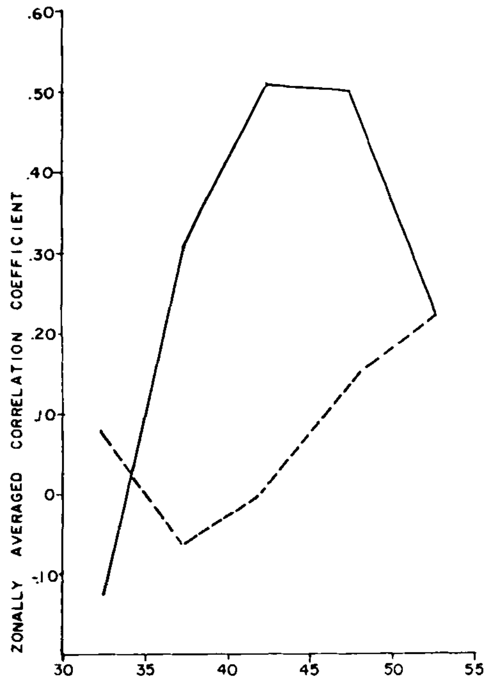

Fig. 2. Zonally averaged (170° E–140° W) correlation between type 2 advection ($W' \cdot \nabla\bar{T}$) and May to summer SST anomaly change. Solid curve is specification (i.e., W' was computed from anomalous summer SLP) while the dashed curve is predictive (i.e., W' was computed from anomalous May SLP).

fact that advection type 1 ($\bar{W} \cdot \nabla T'$) and advection type 3 ($W' \cdot \nabla T'$) in specification relate poorly to the summer SST anomaly field, can be explained by considering the relative magnitude of the components involved. While mean and anomalous currents are of the same order of magnitude, the mean gradient (which is found primarily in the north–south direction) is an order of magnitude greater than the anomalous gradient. As a result, type 2 advection is an order of magnitude greater than types 1 and 3. Apparently the usefulness of type 2 advection for *predictive* purposes is small since May SLP anomalies show small persistence from May to summer in the region of interest.

4. Testing of predictive models of summer SST for the North Pacific

The final portion of this paper is devoted to testing the predictability of summer SST anomalies. Summer SST was predicted in the region 170° E–140° W, 30–55° N using multiple linear regression. The predictand is summer SST at each of 25 boxes (5° latitude by 10° longitude) as shown in Fig. 1. Gridpoint values of SST were available on a 5° × 5° grid. Thus, SST in each box is the average of six gridpoint values. One multiple linear regression equation was used to predict the summer SST anomaly (SSTS) for each box. The potential predictors were May SST anomaly (SSTM), April and May wind frequency parameters from the FNOC data set, and the three components of oceanic thermal advection ($\bar{W} \cdot \nabla T'$, $W' \cdot \nabla\bar{T}$, and $W' \cdot \nabla T'$). It was expected that the best predictor of SSTS at each box would be SSTM. This expectation was supported by the high correlations between SSTM and SSTS (Table 5). Persistence (through the use of SSTM) serves a dual role as both primary predictor and control forecast. In order for the models to have any practical value, they must perform better than persistence.

The six potential predictors that were used to quantify the processes of persistence, wind mixing, and thermal advection were entered into screening multiple regression using the Statistical Analysis System (SAS) MAXR option in the STEPWISE procedure (Helwig and Council, 1979). At each step the predictor with the largest r^2 improvement was added. Examination of the models at each step indicated that after the third predictor was added, the r^2 value failed to increase appreciably with the

Table 5. *Correlations between May and summer SST for each of 25 boxes. Correlations greater than 0.355 (underlined) are significant at the 5% level*

	170° E – 180	180 – 170° W	170° W – 160	160 – 150	150 – 140
55–50	.598	.586	.742	.832	.839
50–45	.540	.642	.749	.832	.749
45–40	.498	.598	.440	.509	.482
40–35	.641	.588	.770	.669	.527
35–30	.419	.339	.574	.640	.662

addition of more predictors. On this basis, it was decided that three predictors would be used in the models.

Model verification was done using a hindcast approach. The entire sample was used to derive equations whose hindcast skill was assessed. Model verification using an independent sample to assess forecast skill was not done because of the small sample that would result from partitioning the data into a dependent and independent sample. While independent testing measures forecast, as opposed to hindcast skill, the hindcast approach enjoys the advantage of a larger sample size.

One statistic used to measure hindcast performance in this study is the canonic skill (Preisendorfer, 1979). The canonic skill (Q) is defined as the ratio

$$Q = \sum \hat{Y}^2 / \sum (Y - \hat{Y})^2 \tag{5}$$

where Y and $\hat{Y}$ are the observed and model predicted values, respectively, of the dependent variable (which is in anomaly form). The summations were carried out over the observations of the dependent sample. The significance of Q can be assessed using the relation:

$$F = (n - p) \cdot Q/p = \nu_2 \cdot Q/\nu_1 \tag{6}$$

The degrees of freedom of the F distribution are ν_2 and ν_1, respectively, where n = sample size, p = number of predictors, $\nu_2 = n - p$, and $\nu_1 = p$. The canonic skill (Q) can be used in two ways. The value of Q is an absolute measure of skill. The greater the value of Q, the greater the explained variance of the dependent variable by the independent variables. However, hindcast skill can be increased by merely increasing the number of predictors. The F statistic accounts for this and is used to assess model significance. The null hypothesis which was tested is that all the regression coefficients are zero. It is possible to find significance (at a high level) with no skill present.

Regression equations containing three independent variables were formed from the pool of six predictors, using the entire 30-year sample (1947–76). The corresponding Q scores (top of Table 6) were found significant at the 5% level for 24 boxes and at the 1% level of 21 boxes. The hypothesis which was rejected with the stated significance is that all the regression coefficients are identically equal to zero. Thus, this is a test of model significance.

It should be noted that because *screening* regression was used, the appropriate value of p lies somewhere between 3 (number of variables selected) and 6 (number of variables in the pool). Since half of the pool of predictors were used, the value of p is much closer to 6 than 3. This conclusion is based on Fig. 1 of Davis (1977) which indicates that the artificial skill (S_A) which results from sampling error (due to the use of a finite sample) and the screening process is much closer to that of a 6- than a 3-variable model. In fact, given a model size (M_S) of 3 and a pool of size of 6 (M) the $\mathcal{F}$ value (the ratio of S_A screening 3 out of 6 variables to S_A for a full 6-variable model) is about 0.87. Thus, $p = 5.5$ (subjectively chosen) was used in the application of the F test for model significance.

In addition to correcting the p value for use in the F test, the sample size (n) was also adjusted using the following formulas given by Sciremammano (1979):

$$n = \frac{N \Delta t}{\tau} \tag{7}$$

Table 6. *Canonic hindcast skill (Q) for three-predictor (top) and SST only (bottom) multiple regression models. Significance at the 5% (+) or 1% (†) level is noted*

	170° E–180	180–170° W	170° W–160	160–150	150–140
55–50	.776*	1.133*	2.616*	3.809*	5.736*
	.590*	.634*	1.520*	2.395*	2.377*
50–45	1.214*	1.855*	1.990*	3.547*	2.256*
	.488*	.788*	1.381*	2.218*	1.253*
45–40	.435†	.882*	.760*	.783*	.685*
	.334*	.508*	.212†	.333*	.300*
40–35	.967*	.662*	1.626*	.956*	.434†
	.635*	.506*	1.526*	.820*	.399*
35–30	.496†	.139	.985*	.983*	.956*
	.220†	.108	.491*	.694*	.809*

$$\tau = \sum_{i=-\infty}^{+\infty} C_{xx}(i\,\Delta t)\cdot C_{yy}(i\,\Delta t)\cdot \Delta t \tag{8}$$

where n = effective sample size, N = actual sample size (30 years), Δt is the frequency of observations in the time series (1 year) and τ is the characteristic time scale of a given predictor with respect to the predictand whose autocorrelation functions are C_{xx} and C_{yy}. In order to estimate n for each model, the τ's for each predictor were averaged. The reason for the computation of n is that due to persistence (autocorrelation) successive values of predictors and predictands are not completely independent (an assumption of the classical F test); the effective sample size n was used in the F test.

It is not at all surprising, considering the high degree of persistence of SST in the region of interest, that any model which utilizes SST as a predictor at short lags will prove to predict significantly better than chance. In fact, when May SST was used alone as a predictor of summer SST (bottom of Table 6), model significance was no less than when three predictors were used. Note that the Q values for the one- and three-predictor models are not comparable. The expected value of Q for the three-predictor model is higher than that for the SSTM only model because it has two additional predictors. Significance levels are directly comparable, however, since the F statistic explicitly accounts for the number of predictors.

The problem of model skill was next assessed for both the three-predictor and SSTM only models. While the three-predictor models are significant for all but one box, what is of practical importance is whether or not the models perform better than persistence (SSTM alone). The absolute measure of skill adopted here is the true skill (Davis, 1976, 1978).

$$S = S_{\rm H} - S_{\rm A} \tag{9}$$

where

$$S_{\rm H} = 1 - \sum (Y - \hat{Y})^2 / \sum Y^2, \tag{10}$$

Y is the predictand (anomaly) and $\hat{Y}$ is the model estimate of Y. The hindcast skill $S_{\rm H}$ is simply the explained variance (r^2) of the model. The artificial predictability ($S_{\rm A}$) that results from imperfect estimates of the model statistics (i.e., sampling error) is given by

$$S_{\rm A} \simeq \sum_{p=1}^{M} \tau_p / N\,\Delta t \tag{11}$$

where M is the number of predictors, N is the sample size, Δt is the frequency of the observations and τ is the characteristic time scale of the model components. The artificial skill $S_{\rm A}$ was estimated from (8) and (11). The screening process was accounted for by computing $S_{\rm A}$ using $M = 5$ and multiplying it ($S_{\rm A}$) by 0.87. This value (0.87) is the $\mathscr{F}$ value from Fig. 1 of Davis (1977) as discussed above.

The values computed for $S_{\rm A}$ vary from box to box. The range of values is 0.03–0.07 and 0.11–0.17 for the one- and three-variable models, respectively. The value of S, computed as the

Table 7. *The true skill* (S) *for the three-predictor* (*top*) *and SSTM only* (*bottom*) *regression models. The values on the right are the latitudinal averages*

Latitude	170°E–180	180–170°W	170°W–160	160–150	150–140	$\bar{S}$
55–50	.29	.38	.53	.59	.62	.48
	.34	.35	.54	.63	.62	.50
50–45	.36	.48	.45	.58	.51	.48
	.28	.40	.54	.63	.48	.48
45–40	.15	.29	.25	.27	.25	.24
	.20	.29	.14	.21	.20	.22
40–35	.30	.21	.43	.30	.15	.28
	.33	.29	.55	.40	.24	.37
35–30	.17	−.05	.32	.34	.31	.22
	.12	.06	.29	.37	.40	.26

difference $S_H - S_A$, is given in Table 7 for the three (top) and one (bottom) predictor models. The interpretation of the true skill (S) is the amount by which the explained variance of the model (S_H) exceeds that expected by chance (S_A). That is, S is a corrected estimate of the hindcast skill of the model. The results in Table 7 show no improvement of the three-predictor models over persistence. It appears that the two additional predictors do not make a significant improvement over persistence; however, this is merely a qualitative assessment.

Next, an overall assessment of the predictability of box-averaged summer SST in the eastern North Pacific was made by examining the statistics in Tables 6–7. In general, the models exhibited considerable hindcast skill and significance. However, this is due mostly to persistence. Still, there are quite high values of skill in the northeast region, particularly for box 5. It was here that the highest correlations between the predictors and summer SST were found. Apparently, most of the useful information possessed by all of the other predictors is also explained by the May SST anomaly (persistence).

5. Discussion and conclusions

In diagnostic analyses, the relationship between oceanic wind mixing and summer SST was investigated at four OWS's (C, D, P and V). The use of OWS data takes advantage of the high quality (i.e., measured wind speed) and frequency of observation (3 hourly) not available elsewhere. The analysis indicates that knowledge of the magnitude of individual (daily) wind events during spring does no better in describing future (summer) SST than the monthly average; the proposed mechanism is deepening of the oceanic mixed layer via wind mixing. Perhaps other factors, such as atmospheric stability, duration of the event, and mixed layer state must be taken into account in order to make full use of knowledge of daily wind forcing to predict SST. The primary approach used here was the correlation of the mean of the daily wind speed raised to powers varying from one to four with the summer SST, holding May SST constant.

In the predictive section of this paper, the wind speeds used were box-averaged values defined from SLP analyses. These had to be used since *measured point* values of wind speed are not available over the domain in which SST was predicted. Both the fact that the winds were derived from SLP (not measured) and were averaged over a large area may have destroyed much of the predictive information they contain. No good relationship between the area-averaged wind parameters and summer SST was found. In contrast, the correlations derived at the OWS's were based on measured, point values of wind speed. The results at OWS P suggest that a lag effect may be in operation, since significant (negative) correlations between wind speed and SST remained even after the contemporaneous effect was removed.

Computations of oceanic thermal advection were used to show the relative importance of the three components of the total advection. When the anomalous summer currents were used (i.e., specification), it was found that type 2 advection ($\mathbb{W}' \cdot \nabla\bar{T}$) was the dominant term. This is especially true at 40–50° N. In fact, the 30-year mean pattern correlation between ($\mathbb{W}' \cdot \nabla\bar{T}$) and May to summer SST anomaly change is about the same as that of persistence ($r \sim 0.4$) between 40 and 50° N. The other two terms ($\bar{\mathbb{W}} \cdot \nabla T'$ and $\mathbb{W}' \cdot \nabla T'$) are an order of magnitude smaller than $\mathbb{W}' \cdot \nabla\bar{T}$. The dominance of $\mathbb{W}' \cdot \nabla\bar{T}$ is due to the very large long-term mean north–south SST gradient between 40 and 50° N. Certainly, the primary contribution to $\mathbb{W}' \cdot \nabla\bar{T}$ is through the meridional component of the anomalous surface current. The dominance of $\mathbb{W}' \cdot \nabla\bar{T}$ in this study confirms what has been found in the past for *limited samples* on a case study basis by others such as Namias (1959 and 1965), Jacob (1967), Clark (1972), Haney *et al.* (1978), and Haney (1980). Unfortunately, due to small persistence of the atmospheric flow (and, thus, wind-induced currents), the importance of $\mathbb{W}' \cdot \nabla\bar{T}$ is greatly diminished when anomalous *May* currents are used for summer SST prediction.

The multiple linear regression models formulated to predict box-averaged summer SST anomaly performed well enough to suggest only a marginal improvement over persistence; strictly speaking, the level of statistical significance is unknown. Thus, neither wind mixing (as parameterized here) nor oceanic thermal advection had very much overall *predictive* value. However, persistence alone results in generally moderate to large values of skill.

While the results of the predictive aspects of this paper are disappointing it should be kept in mind that the approach used here was by design a simple one. Only some of the important physical processes were included; the parameterizations of those processes included avoided many details which would have added greater expense and which may have precluded their use in real time forecasting due to the absence of data.

In particular, the wind data was utilized in order to render proxy information regarding the character of the oceanic mixed layer. Such an approach was taken because of the spatial and temporal sparsity of bathythermograph observations. In addition to data deficiencies, this study has pointed out deficiencies in our understanding of the atmospheric system. We are lead to a dismaying circular argument when we try to predict SST fields for use in long-range atmospheric forecasts. In order to predict the oceanic state (SSTS), we must first improve long-range atmospheric predictions (since future winds are needed to carry out advective calculations which explain much of the evolution of the SST field).

6. Acknowledgments

New Jersey Agricultural Experiment Station, Publication No. D-13405-2-82, supported by State funds (Project 13405) and by the Climate Dynamics Program, Division of Atmospheric Sciences, National Science Foundation, under Grant ATM-8023136.

We wish to acknowledge the many persons who have assembled and disseminated the data sets which were used here, and those who have aided us in the use of the computer. The suggestions provided by Drs. James R. Miller and Nathan M. Reiss are appreciated. Also, we wish to thank Ms. Ruth Smith and Ms. Valerie Bowers for typing this manuscript.

REFERENCES

Adem, J. 1970. Incorporation of advection of heat by mean winds and by ocean currents in a thermodynamic model for long-range weather prediction. *Mon. Wea. Rev. 98*, 776–786.

Adem. J. 1970. On the prediction of mean monthly ocean temperature. *Tellus 22*, 410–430.

Arthur, R. S. 1966. Estimation of mean monthly anomalies of sea-surface temperature. *J. Geophys. Res. 71*, 2689–2690.

Barnett, T. P. 1978. The role of the oceans in the global climate system. In *Climatic change*. Chapter 10, Cambridge University Press.

Bathen, K. H. 1972. On the seasonal changes in the depth of the mixed layer in the North Pacific Ocean. *J. Geophys. Res. 77*, 7138–7150.

Brooks, C. E. P. and Carruthers, N. 1978. *Handbook of statistical methods in meteorology*. London: Her Majesty's Stationery Office, 245–254.

Budyko, M. 1955. *Heat balance atlas*. U.S. Dept. of Commerce, no. TT63-13243.

Camp, N. T. and Elsberry, R. L. 1978. Oceanic thermal response to strong atmospheric forcing, II. The role of one-dimensional processes. *J. Phys. Oceanogr. 8*, 215–224.

Clark, N. E. 1972. Specification of sea surface temperature anomaly patterns in the eastern North Pacific. *J. Phys. Oceanogr. 2*, 391–404.

Davis, R. E. 1976. Predictability of sea surface temperature and sea level pressure anomalies over the North Pacific Ocean, *J. Phys. Oceanogr. 6*, 249–266.

Davis, R. E. 1977. Techniques for statistical analysis and prediction of geophysical fluid systems. *Geophys. Astrophys. Fluid Dyn. 8*, 245–277.

Davis, R. E. 1978. Predictability of sea level pressure anomalies over the North Pacific Ocean. *J. Phys. Oceanogr. 8*, 233–245.

Dept. of the Navy Oceanographic Office 1977. *Surface Currents/North Central Pacific Ocean.* Washington, D.C., Spec. Pub. 1402 NP8.

Dept. of the Navy Oceanographic Office 1977. *Surface Currents/Gulf of Alaska.* Washington, D.C., Spec. Pub. 1402-NP6.

Dept. of the Navy Oceanographic Office 1977. *Surface Currents/North Central North Pacific Ocean.* Washington, D.C., Spec. Pub. 1402-NP8.

Dept. of the Navy Oceanogrpahic Office 1977. *Surface Currents/Northeast North Pacific Ocean Including the West Coast of the United States.* Washington, D.C., Spec. Pub. 1402-NP9.

Eber, L. E. 1961. Effects of wind-induced advection on sea surface temperature. *J. Geophys. Res. 66*, 839–844.

Elsberry, R. L. and Camp, N. T. 1978. Oceanic thermal response to atmospheric forcing, I. Characteristics of forcing events. *J. Phys. Oceanogr. 8*, 206–214.

Elsberry, R. L. and Garwood, R. W. 1978. Sea-surface temperature anomaly generation in relation to atmospheric storms. *Bull. Amer. Meteorol. Soc. 59*, 786–789.

Elsberry, R. L. and Raney, S. D. 1978. Sea-surface temperature response to variations in atmospheric wind forcing. *J. Phys. Oceanogr. 8*, 881–887.

Haney, R. L. 1980. A numerical case study of the development of large-scale thermal anomalies in the central North Pacific Ocean. *J. Phys. Oceanogr. 10*, 541–556.

Haney, R. L., Shiver, W. S. and Hunt, K. H. 1978. A dynamic-numerical study of the formation and evolution of large-scale ocean anomalies. *J. Phys. Oceanogr. 8*, 952–969.

Helwig, J. T. and Council, K. A. 1979. *SAS user's guide.* SAS Institute, Inc., Raleigh, 494 pp.

Jacob, W. J. 1967. Numerical semiprediction of monthly mean sea surface temperature. *J. Geophys. Res. 72*, 1681–1689.

Namias, J. 1959. Recent seasonal interactions over the northern Pacific from summer 1962 through the subsequent winter. *J. Geophys. Res. 64*, 631–646.

Namias, J. 1965. Macroscopic associations between mean monthly sea-surface temperature and the overlying winds. *J. Geophys. Res. 70*, 2307–2318.

Namias, J. 1972. Experiments in objectively predicting some atmospheric variables for the winter of 1971–1972. *J. Appl. Meteorol. 11*, 1164–1174.

Namias, J. 1976. Negative ocean-air feedback systems over the North Pacific in the transition from warm to cold seasons. *Mon. Wea. Rev. 104*, 1107–1121.

Preisendorfer, R. W. 1979. Model skill and model significance in linear regression hindcasts. Scripps Institution of Oceanogrpahy Reference Series, La Jolla, CA,, No. 79–12.